Development of a mathematical model of dynamic soil deformation taking into account the variable coefficient of volumetric viscosity

Natalya Remez[1], *Hennadii* Haiko[1*], *Alina* Dychko[2], *Viktor* Boiko[3], *Svitlana* Haiko[4], and *Olena* Antoniuk[5]

[1]National Technical University of Ukraine "Igor Sikorsky Kyiv Polytechnic Institute", 37 Beresteiskyi Ave., 03056 Kyiv, Ukraine
[2]Taurida National V.I. Vernadsky University, 33 Dzhona Makkeina St., 01042 Kyiv, Ukraine
[3]Institute of Hydromechanics of the National Academy of Sciences of Ukraine, 8/4 Marii Kapnist St., 03057 Kyiv, Ukraine
[4]Institute of Telecommunications and Global Information Space, 25 Chokolivskyi Ave., 03186 Kyiv, Ukraine
[5]Ukrainian State University of Science and Technologies, 4 Nauky Ave., 49600 Dnipro, Ukraine

Abstract. Determining soil deformations under the influence of dynamic loads of different nature, including during military actions, is an important scientific and practical problem. At the same time, when solving problems of determining the stress-strain state of soils under the action of short-term dynamic loads, little attention has been paid to the multicomponent composition and viscous properties. The aim of the research is to develop a mathematical model of soil deformation taking into account the variable coefficient of volumetric viscosity both during loading and unloading. The methods of mathematical modeling and numerical integration are used in the research. The possibility of using the proposed model to determine the deformation of soils under explosive and shock loads is shown, which helps control the properties of soils for the protection of shallow underground structures. The results of a comparison of the obtained analytical data with the experimental data are presented.

1 Introduction

For a long time, Europe lacked a doctrine for large-scale war involving modern conventional weapons [1]. This absence of a comprehensive strategy led to significant oversight in the planning and project decisions of shallow underground complexes. The security (protective) factor was not given priority in these decisions. Consequently, these structures were designed without considering potential military threats [2]. The absence of a clear strategy meant that security considerations were often overlooked. As a result, open cast and shallow underground complexes were not adequately protected against modern military risks [3]. This oversight highlights the need for a revised approach to planning and designing these structures.

* Corresponding author: h.haiko@kpi.ua

However, the current increase in military risks has changed this perspective. Now, there is a growing recognition of the importance of security considerations in these planning processes [4]. As a result, research into these issues, which are both science-intensive and far from theoretical, has become a priority. These research efforts aim to address practical solutions for enhancing the protection of such underground complexes [5]. The urgency and importance of this research reflect the modern conditions and the need for effective security measures.

World and local experience of underground space development demonstrate that ensuring the reliability and safety of underground infrastructure objects from dynamic loads is a significant challenge [3, 6]. This problem is science-intensive and cannot be solved solely through natural experiments [7]. The complexities involved require a more comprehensive approach. Under conditions of war and terrorist threats, the relevance of protecting shallow underground structures becomes even more critical [1, 4, 8]. The role of the geological environment surrounding the underground facility in providing protection is increasingly recognized. Effective and economically justified approaches to addressing these challenges are essential. These solutions are mainly implemented based on appropriate mathematical models, which provide the necessary precision and reliability [4, 9]. Modern concepts demand the use of mathematical models throughout the entire lifecycle of an object [10]. These models are essential during the planning stage to ensure precise design specifications[11]. They play a crucial role during construction and continue to be vital in the operation phase for maintaining and optimizing performance [12]. The soil massif and its protective properties remain the key element in this project. Its ability to absorb and dissipate dynamic loads is crucial for the safety of underground structures [10, 13]. This importance underscores the need for precise mathematical models that accurately represent soil deformation under such conditions [14]. Adequate approximation of these models to real processes is essential. When these models effectively simulate the impact of dynamic loads, such as explosions from air attacks, they provide valuable insights. These insights open new possibilities for innovative design solutions [1, 15]. Consequently, the enhanced models can significantly improve the protection of underground objects, ensuring their resilience and safety.

2 Literature review

The rheological properties of soils are of great importance in understanding soil behaviour. Properties such as creep play a critical role in how soils deform over time. Stress relaxation is another key property, indicating how soils gradually reduce stress under a constant strain [16, 17]. Long-term strength is vital for assessing soil stability over extended periods. These rheological properties are closely related to the viscosity of the soil. Viscosity itself influences how soils flow and resist deformation [16, 18]. To study these properties, different models can be employed. Well known approach involves analysing wave processes in soils [19].

Another method uses the similarity theorem to draw parallels between different rheological phenomena [20, 21]. Additionally, machinery learning techniques can be applied for more accurate predictions [22]. Neuron networking offers a sophisticated way to model complex soil behaviours [23]. Other AI methods of modelling can also be utilized to enhance our understanding of soil rheology [24]. Each of these methods contributes to a more comprehensive analysis of soil properties.

The rheological properties of soils, including creep, stress relaxation, and long-term strength, are closely related to the viscosity of the soil itself. Viscosity plays a crucial role in determining how soils behave under various stress conditions. In soil mechanics, the concept of viscosity is fundamental and cannot be overlooked [25]. Any rheological model

used to analyse soil behaviour invariably incorporates the simplest Newtonian model. This model serves as a foundation for understanding more complex behaviours exhibited by soils under different loading conditions.

Currently, there is a fairly large number of mechanical models that describe the rheological properties of the soil skeleton. These models are constructed by combining elastic, viscous, and plastic elements to capture the complex behavior of soils. The properties of the soil skeleton are represented through various models. One such model is the Kelvin-Voigt model, which incorporates both elasticity and viscosity [26]. Well-known model is the Maxwell model, which combines viscous flow and elastic deformation [27]. Additional models include the Shvedov model, the modified Tymoshenko model, and the Bingham-Shvedov-Maslov model, each offering unique insights into the rheological properties of soils [26 – 28].

The Modified Tymoshenko model is a significant tool in soil mechanics for describing angular viscoplastic deformation. This model is particularly useful in understanding the speed of such deformations under various conditions. Z.G. Ter-Martirosyan applied this model to analyze creep deformations. The focus was on how these deformations occur during shear stress applied to the soil medium. By using the Modified Tymoshenko model, Ter-Martirosyan was able to capture the complexities of soil behavior under shear. This application provides valuable insights into the long-term stability and performance of soil structures [28, 29].

The resulting rheological equation for clayey soils is a complex and nuanced representation of their behavior. This equation accounts for both the simultaneous hardening and softening that occur during the shear process. The intricate nature of this phenomenon has been extensively studied by several prominent researchers. It was made significant contributions to understanding the hardening aspects of clayey soils and provided insights into the softening mechanisms that accompany shear stress [30]. S.R. Meschyan's work further elaborated on the interplay between hardening and softening [26, 27, 31]. It was contributed valuable experimental data supporting these theories [32]. G.Y. Ter-Stepanyan introduced additional modifications to the rheological models. Z.G. Ter-Martirosyan integrated these findings into a comprehensive rheological equation [29]. Collectively, their works provide a robust framework for predicting the behavior of clayey soils under shear stress[26, 27, 32 – 34].

Because the soil viscosity coefficient depends on many factors, such as time, the stress-strain state of the soil mass, temperature, humidity, re-arrangement of soil particles during its compaction and creep, the determination of this parameter during experimental studies and subsequent interpretation of the obtained results, based on different test methods, is difficult and leads to a wide spread of results [35].

In most cases, there is a misinterpretation of the value itself. Indeed, taking viscosity as a constant value (η = const) is valid only for an ideally viscous (Newtonian) medium. In soils, the correlation between stresses and flow speed is nonlinear, and because of this, the coefficient of soil viscosity will be a variable value, depending both on the magnitude of the applied load and on the time of its action.

So, for example, at the beginning of the test, when the soil deformations are still small, the soil viscosity can be 10^{13} Poise, and closer to the end of the deformation stage, the value of the viscosity coefficient can increase to a value of 10^{14} Poise. This phenomenon is confirmed in [36] based on experimental studies on sandy soils.

The viscosity coefficient is also used to describe the nature of the deformation of ice, thawed and frozen soil [37]. The average values of the viscosity of ice, depending on its structure, temperature, and the load acting on it, are in the range from 10^{10} to 10^{15} Poise [38]. The research [39] summarizes the viscous properties or the influence of the speed of loading on the behavior of stress and deformation of unbound and bound soils, in particular

unbound granular materials. Viscous properties are evaluated by gradually changing the speed of deformation and performing a long-term load during another monotonous load. However, the work emphasizes that any constitutive model that describes the influence of the load speed as a function of time is not objective.

The research [40, 41] proposes a mathematical model that allows estimating the total, elastic, and final deformations that occur in soils of complex composition under the action of short-term force loading. In the research, the multicomponent composition of the soil is not taken into account, and the limit diagrams of compression and unloading are assumed to be linear.

In the research [42] the spread of waves in the soil within the framework of an elastic-viscoplastic medium with a constant viscosity coefficient is considered.

Currently, the most advanced model of water unsaturated soils, which takes into account their multicomponent and viscous properties, is the model of a solid multicomponent viscoplastic medium [37].

3 Research methods

In the study of the action of an explosive pulse on the soil environment, extended modes of loading were analyzed to understand their impact. The mathematical approach involved deriving a second-level differential equation. This differential equation is crucial for modeling the dynamic response of the soil to explosive forces. To solve this complex equation, the Runge-Kutta method of the fourth order was employed. This numerical technique is known for its accuracy in solving differential equations. The use of the Runge-Kutta method allowed for precise simulations of soil behavior under explosive loading conditions [38].

To approximate the system of differential equations that describe the spread of explosive waves in the soil, the finite difference method using a finite difference scheme of the “cross” type of the second order of accuracy in space and time coordinates is used. Mobilegrid that automatically expands to size of spread of shock wave is applied in the solution. As an additional value to the average hydrostatic pressure of movement the linear-quadratic artificial viscosity is entered inequation of differences that allows to make through calculations, both on smooth and discontinuous ones flows [38].

As experimental studies demonstrate [43], with increasing loading speed, the viscosity coefficient of soils η decreases. The decision of the question of how to introduce variable viscosity for soils is under development currently.

The constitutive correlations of the model include the equation of volumetric compressibility and unloading of the medium

$$F(P,\ \dot{P},\ \varepsilon,\ \dot{\varepsilon}) = 0 \tag{1}$$

and the plasticity condition proposed for soils by A.I. Botkin and S.S. Grigoryan [37] as following

$$\begin{gathered} T = \sqrt{6} I_2 = F\left(P\right); \\ I_2 = \frac{1}{6}\left[\left(\sigma_1 - \sigma_2\right)^2 + \left(\sigma_2 - \sigma_3\right)^2 + \left(\sigma_3 - \sigma_1\right)^2\right], \end{gathered} \tag{2}$$

where P is the average hydrostatic pressure; ε is the volumetric deformation of medium; $\dot{P},\ \dot{\varepsilon}$ are their time derivatives; T is the intensity of tangential stresses; $\sigma_1,\ \sigma_2,\ \sigma_3$ are main normal stresses.

The presence of time derivatives of pressure and strain in equation (1) makes it possible to take into account the influence of deformation speed on the nature of deformation.

Dependence (1) is different at loading and unloading, which causes the appearance of residual deformations. At $\dot{P} \to \infty,\ \dot{\varepsilon} \to \infty$ – the equation of limiting dynamic compression is follows, and at $\dot{P} \to 0,\ \dot{\varepsilon} \to 0$ – the equation of limiting static compression of the medium.

The model of medium takes into account the effect of deformation speed on volume change only, and landslide viscosity is not taken into account. Volumetric deformation and deformation speed are related to the deformation and deformation speed of the components by the correlations

$$\varepsilon = \sum_{i=1}^{3} \alpha_i \varepsilon_i,\ \ \dot{\varepsilon} = \sum_{i=1}^{3} \alpha_i \dot{\varepsilon}_i, \tag{3}$$

where α_1 is the content of pore space, α_2 is the content of liquid component, α_3 is the content of solid components – per unit volume of soil, and $\alpha_1 + \alpha_2 + \alpha_3 = 1$.

It is accepted that the equation of dynamic volumetric compression of a medium $P_D - P_0 = f_D(\varepsilon)$ differs from the equation of static volumetric compression $P_S - P_0 = f_S(\varepsilon)$ by a linear term $P_D(\varepsilon) - P_S(\varepsilon) = k\varepsilon$ (k – proportionality coefficient).

Taking these assumptions into account, the equation of dynamic volumetric compression of a solid porous multicomponent viscoplastic medium can be written as

$$\dot{\varepsilon} = \left(\frac{\alpha_1}{\dfrac{df_D}{d\varepsilon_1}} + \sum_{i=2}^{3} \alpha_i \frac{dg_i}{dP} \right) \dot{P} - \frac{\alpha_1}{\eta(\varepsilon)} \left(1 - \frac{\dfrac{df_S}{d\varepsilon_1}}{\dfrac{df_D}{d\varepsilon_1}} \right) \left\{ P - P_0 - f_S \left[\left(\varepsilon - \sum_{i=2}^{3} \alpha_i \varepsilon_i \right) \frac{1}{\alpha_1} \right] \right\}, \tag{4}$$

where $\varepsilon_i = g_i(P)$ is the compression diagrams of solid and liquid components (they are the same for both dynamic and static loading, since it is assumed that under the action of short-term and long-term loading the deformation of solid and liquid components is the same); $\eta(\varepsilon)$ is the variable coefficient of volumetric viscosity of medium.

One of the most well-known types of equations for dynamic and static compression of media (metals, rocks, water, air) is the Theta equation. The constants included in this equation have a specific physical meaning.

Let us consider a variant of the model when the compression equation of liquid and solid components are Theta type equations. Then equation (4) becomes as following

$$\dot{\varepsilon} = \varphi(P,\ \varepsilon)\dot{P} - \frac{\alpha_1 \lambda(P,\ \varepsilon)}{\eta(P,\ \varepsilon)} \psi(P,\ \varepsilon). \tag{5}$$

The functions included in the equation (5) for the load are the following.

Under load:

$$\varphi(p,\ \varepsilon) = \alpha_1 \left(\frac{d f_D}{d\varepsilon_1} \right)^{-1} - \sum_{i=2}^{3} \alpha_i B_i \left[A_i (p - p_0) + 1 \right]^{-k_i - 1};\ \lambda_1(p,\ \varepsilon) = 1 - \left(\frac{df_D}{d\varepsilon_1} \right)^{-1} \frac{df_s}{d\varepsilon_1};$$

$$\psi(p,\ \varepsilon) = p - p_0 - f_s(\varepsilon_1);\ f_s(\varepsilon_1) = A_s^{-1} \left[(\varepsilon_1 + 1)^{-\gamma_s} - 1 \right];\ f_D(\varepsilon_1) = f_s(\varepsilon_1) + k_{\varepsilon_1};\ \kappa < 0;$$

$$\varepsilon_1 = \frac{1}{\alpha_1} \left(\varepsilon - \sum_{i=1}^{3} \alpha_i \varepsilon_i \right) = \frac{1}{\alpha_1} \left\{ \varepsilon + 1 - \sum_{i=1}^{3} \alpha_i \left[A_i (p - p_0) + 1 \right]^{-k_i} \right\} - 1;\ A_i = \frac{\gamma_i}{\rho_{i_0} c_{i_0}^2}; \tag{6}$$

$$B_i = \frac{1}{\rho_{i_0} c_{i_0}^2};\ k_i = \frac{1}{\gamma_i};\ i = 2,\ 3;\ A_s = \frac{\gamma_s}{\rho_0 c_s^2}.$$

In the equation (6) the following notations are used: ρ_{i_0}, c_{i_0} are density and speed of sound of liquid and solid components at atmospheric pressure P_0; γ_i is the exponents in Theta type equations for these components; ρ_0 is the initial density of the medium at P_0; c_s, γ_s are speed of sound and exponent in the equation of volumetric compression under static loading.

The model assumes that the equations for unloading the material of the solid and liquid components coincide with the equations for their loading.

Unloading of free pore space occurs according to the following equation

$$\varepsilon +1=\left[\frac{\gamma_S(P_m-P_0)}{\rho_0 c_S^2}+1\right]^{-1/\gamma_S}-\left[\frac{\gamma_{SR}(P_m-P_0)}{\rho_0 c_{SR}^2}+1\right]^{-1/\gamma_{SR}}, \tag{7}$$

where c_{SR} is the speed of sound when medium is unloaded; γ_{SR} is the exponent in the equations of volumetric compression during unloading of medium; P_m is the pressure when the volumetric deformation of the pore space reaches its maximum value ε_{1m}.

Unloading of medium occurs when deformation ε_1 reaches the value ε_{1m}, that is, when it is met the condition

$$\dot{\varepsilon}=\frac{1}{\alpha_1}\left(\dot{\varepsilon}-\sum_{i=2}^{3}\alpha_i\varepsilon_i\right)=\frac{1}{\alpha_1}\left[\frac{\dot{V}}{V_0}-\sum_{i=2}^{3}B_i\left(A_i(P-P_0)+1\right)^{\frac{-(1+\gamma_i)}{\gamma_i}}\dot{P}\right]=0. \tag{8}$$

From condition (8) and when $\varepsilon_1=\varepsilon_{1m}$ it is possible to determine P_m:

$$P_m=P_0+A_S^{-1}\left[\left(1+\varepsilon_{1m}\right)^{-\gamma_S}-1\right]. \tag{9}$$

The equation for volumetric unloading of a medium is as (5), but the functions included in it during unloading differ from the corresponding ones during loading and are written as the following:

$$\begin{gathered}
\varphi(p,\ \varepsilon)=\alpha_1\left[\frac{df_D}{d\varepsilon_1}-\frac{df_s}{d\varepsilon_1}+\frac{df_{SR}}{d\varepsilon_1}\right]^{-1}-\sum_{i=2}^{3}\alpha_i B_i\left[A_i(p-p_0)+1\right]^{-k_i-1};\\
\lambda_1(p,\varepsilon)=\left(\frac{df_D}{d\varepsilon_1}-\frac{df_S}{d\varepsilon_1}\right)\left(\frac{df_D}{d\varepsilon_1}-\frac{df_S}{d\varepsilon_1}+\frac{df_{SR}}{d\varepsilon_1}\right)^{-1};\ \psi(p,\varepsilon)=-p-p_0-f_s(\varepsilon_1);\\
f_s(\varepsilon_1)=A_s^{-1}\left[(\varepsilon_1+1)^{-\gamma_s}-1\right];\ f_D(\varepsilon_1)=f_s(\varepsilon_1)+k_{\varepsilon_1};\ \kappa<0;\\
f_{SR}(\varepsilon_1)=A_{SR}^{-1}\left\{\left\{\varepsilon_1+1+\left[A_{SR}\left(p_m-p_o\right)+1\right]^{\frac{-1}{\gamma_{SR}}}-\left[A_S(P_m-P_0)+1\right]^{\frac{-1}{\gamma_S}}\right\}^{-\gamma_{SR}}-1\right\};\\
p_m-p_0=A_S^{-1}\left(\varepsilon_{1m}+1\right)^{-\gamma_S};\ k_i=\frac{1}{\gamma_i};\ i=2,\ 3;\ A_{SR}=\frac{\gamma_{SR}}{p_0 c_{SR}^2};\ A_S=\frac{\gamma_S}{\rho_0 c_S^2}.
\end{gathered} \tag{10}$$

The type of the function for a variable viscosity coefficient $\eta(\varepsilon)$ is determined from the following considerations. For a given soil, there are limiting static P_S and dynamic P_D, as well as intermediate compression diagrams. The higher the loading speed, the closer the compression curve is to the limiting dynamic diagram. Taking these considerations into account, for a given fixed pressure P^*:

$$P^* - P_0 = P_S(\varepsilon_1) + \kappa\varepsilon_1 = \frac{\rho_0 c_S^2}{\gamma_S}\left[(\varepsilon_1+1)^{-\gamma_S} - 1\right] + \kappa\varepsilon_1;\ \kappa < 0;\ |\kappa| \le |k|. \quad (11)$$

The limiting case $\kappa = 0$ corresponds to the static diagram, and $\kappa = k$ is the limiting dynamic diagram. $|\kappa|$ increase corresponds to an increase in loading speed. Taking into account the above, as well as the experimental fact that the viscosity coefficient decreases with increasing loading speed, the following form of the viscosity function is proposed:

$$\eta(\varepsilon) = \eta_D \left(\frac{\kappa - \rho_0 c_S^2}{k - \rho_0 c_S^2}\right)^{-m};\ m > 1, \quad (12)$$

where η_D is the "dynamic" coefficient of volumetric viscosity, corresponding to the value of the function $\eta(\varepsilon)$ at the dynamic diagram.

Having determined the value κ from (11) and substituting its value into (12):

$$\eta(\varepsilon) = \eta_D \left\{\frac{P - P_0 - \frac{\rho_0 c_S^2}{\gamma_S}\left[\gamma_S\varepsilon_1 - 1 + (\varepsilon_1+1)^{-\gamma_S}\right]}{\varepsilon_1\left(k - \rho_0 c_S^2\right)}\right\}^{-m}. \quad (13)$$

From the correlation (13) it follows that the coefficient of volumetric viscosity is a function of the magnitude of volumetric deformation, which depends, in turn, on time, loading modes, pressure, physical and mechanical characteristics of the medium.

The model assumes that during unloading the coefficient of volumetric viscosity is constant and equal to the value achieved at maximum deformation of the medium, that is

$$\eta_R = \eta_D \left\{\frac{P_m - P_0 - \frac{\rho_0 c_S^2}{\gamma_S}\left[\gamma_S\varepsilon_{1m} - 1 + (\varepsilon_{1m}+1)^{-\gamma_S}\right]}{\varepsilon_{1m}\left(k - \rho_0 c_S^2\right)}\right\}^{-m}. \quad (14)$$

However, as theoretical and experimental research demonstrate, at the medium unloading, such time-dependent parameters as pressure and volumetric deformation change. Therefore, the postulate about the constancy of the coefficient a of the volumetric viscosity during unloading is a significant simplification.

In [44 – 46], the behavior of different types of soils is studied within the framework of this model in different loading modes: maximum pressure under load, time of action of the pressure pulse, and time of pressure rise to maximum.

4 Results and discussion

Using the described methods, the research of the effect of volumetric deformation on the volumetric viscosity coefficient is carried out. The research is carried out with the following loading mode parameters: $P_{\max} = 10^5 - 10^9$ Pa; $\Theta = 10^{-2} - 1$ s; $t_{\max} = (0.01 - 0.5)\Theta$. The following designations are used here: $P_{\max}$ is the maximum pressure; Θ is the duration of the pressure pulse; $t_{\max}$ is the time for pressure to rise to maximum.

In Figs. 1 – 3 the dependence of the coefficient of volumetric viscosity on the volumetric deformation of the soil at the same $P_{\max} = 10^6$ Pa and various loading speeds is presented. Curves 1 correspond to the loading speed $\dot{P} = 10^9$ Pa·s, curves 2 – to $\dot{P} = 2 \cdot 10^8$ Pa·s.

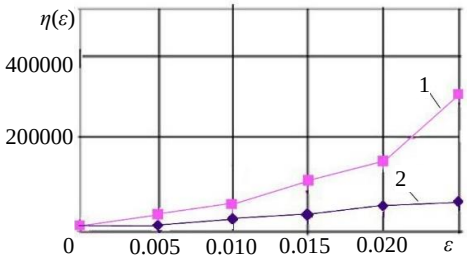

Fig. 1. The dependence of the coefficient of volumetric viscosity on volumetric deformation at $\eta_D = 10^2$ Pa·s.

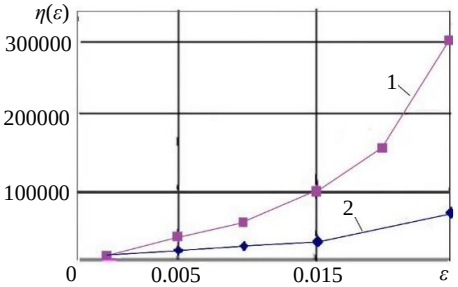

Fig. 2. The dependence of the coefficient of volumetric viscosity on volumetric deformation at $\eta_D = 10^3$ Pa·s.

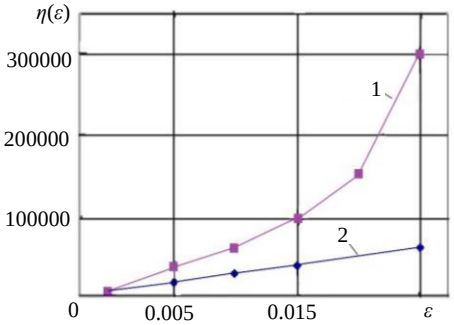

Fig. 3. The dependence of the coefficient of volumetric viscosity on volumetric deformation at $\eta_D = 10^4$ Pa·s.

From the analysis of the figures, it follows that at different values of the dynamic coefficient in viscosity, which corresponds to different types of soils, the same patterns are observed. With an increase in volumetric deformation, the coefficient of viscosity increases, and with an increase in the loading speed, $\eta(\varepsilon)$ decreases.

In Fig. 4 the dependence of the coefficient of volumetric viscosity on the volumetric deformation of soil at loading speed $\dot{P} = 10^9$ Pa/s and at various maximum pressures: 1 – $P_{\max} = 10^5$ Pa, 2 – $P_{\max} = 10^6$ Pa, 3 – $P_{\max} = 10^7$ Pa are presented.

From the analysis of the figure, at the same loading speed $\dot{P} = 10^9$ Pa/s and the same value, the nature of the change in the coefficient of volumetric viscosity at different values of the maximum pressure is different. At the initial stage of loading, the determining role is played by pressure: the greater it is, the faster the maximum deformation is achieved, and, consequently, the coefficient of volumetric viscosity. With a subsequent increase in volumetric deformation, this pattern changes: the highest values $\eta(\varepsilon)$ are achieved at lower values $P_{\max}$.

In all figures it can be observed that the value $\eta(\varepsilon)$ can vary on several orders of magnitude. Hence the conclusion follows that even when the medium is unloaded, the coefficient of volumetric viscosity cannot remain constant. It can be concluded based on the following assumptions.

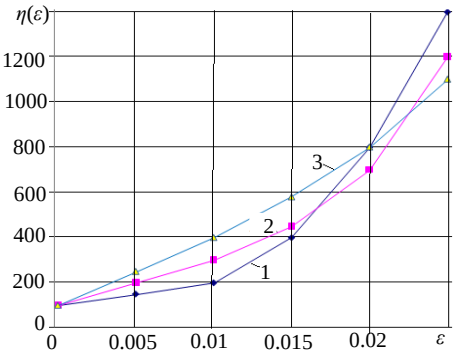

Fig. 4. The dependence of the coefficient of volumetric viscosity on volumetric deformation at $\eta_D = 10^4$ Pa·s and different maximum pressures: 1 – $P_{max} = 10^5$ Pa, 2 – $P_{max} = 10^6$ Pa, 3 – $P_{max} = 10^7$ Pa.

It is assumed that during unloading, the intermediate unloading diagrams are between the limiting static P_{SR} and dynamic P_{DR} diagrams, and the greater the unloading speed, the closer the curve is to the limiting dynamic diagram. Then for a given fixed pressure P^* it can be written

$$P^* - P_0 = P_{SR}(\varepsilon_1) + \kappa\varepsilon_1 = A_{SR}^{-1}\left\{\left\{\varepsilon_1 + 1 + \left[A_{SR}\left(P_m - P_o\right) + 1\right]^{-\gamma_{SR}} - \right.\right.$$
$$\left.\left. = -\left[A_S\left(P_m - P_0\right) + 1\right]^{\frac{-1}{\gamma_S}}\right\} - 1\right\} + \kappa\varepsilon_1,\ \kappa < 0,\ |\kappa| \le |k|. \tag{15}$$

Taking into account formulas (9) and (12) for the coefficient of volumetric viscosity during unloading, the following expression can be obtained

$$\eta(\varepsilon) = \eta_D \left\{ \frac{P - P_0 - A_{SR}^{-1}\left\{\left\{\varepsilon_1 + 1 + \left[A_{SR}/A_S(\varepsilon_{1m}+1)^{-\gamma_S} + 1\right]^{-\gamma_{SR}} - \left[(\varepsilon_{1m}+1)^{-\gamma_S} + 1\right]^{-\gamma_S}\right\}^{-\gamma_S} - 1\right\}}{\varepsilon_1(k - A_{SR}^{-1})} \right\}^{-m}.$$

Let us enter the notations:

$$D_{SR=}\left[A_{SR}/A_S(\varepsilon_{1m}+1)^{-\gamma_S} + 1\right]^{-\gamma_{SR}},\quad D_{SR=}\left[(\varepsilon_{1m}+1)^{-\gamma_S} + 1\right]^{-\gamma_S}.$$

Then for the variable coefficient of viscosity during unloading, it can be written the following expression

$$\eta(\varepsilon) = \eta_D \left\{ \frac{P - P_0 - A_{SR}^{-1}\left\{\left\{\varepsilon_1 + 1 + D_{SR} - D_S\right\}^{-\gamma_S} - 1\right\}}{\varepsilon_1(k - A_{SR}^{-1})} \right\}^{-m}. \tag{16}$$

For comparison with experimental data, numerical modeling of the camouflage action of explosions of a cylindrical charge of TNT is performed. It is assumed that a cylindrical

charge of an explosive substance, which detonates instantly, of infinite length and radius r_0 is placed in the soil space far from the surface, and the same average pressure is established throughout its volume P_{av}, and the density of the explosion products is equal to the initial density of the explosive substance. The movement of soil explosion products is described by the laws of saving of impulse, mass and internal energy, which for the explosion of a cylindrical charge is as following [44, 45]:

$$\frac{\partial \sigma_{rr}}{\partial z} + \frac{\partial \tau_{rz}}{\partial r} + \frac{\tau_{rz}}{r} = \rho \frac{du}{dt}; \tag{17}$$

$$\frac{\partial \tau_{rz}}{\partial z} + \frac{\partial \sigma_{zz}}{\partial r} + \frac{\sigma_{zz} - \sigma_{\theta\theta}}{r} = \rho \frac{dw}{dt}; \tag{18}$$

$$\frac{1}{V}\frac{dV}{dt} = \frac{\partial u}{\partial z} + \frac{\partial w}{\partial r} + \frac{w}{r},\ V = \frac{\rho_0}{\rho}; \tag{19}$$

$$u = \frac{dz}{dt},\ \ w = \frac{dr}{dt}; \tag{20}$$

$$\sigma_{zz} = S_{zz} - P,\ \sigma_{rr} = S_{rr} - P,\ \sigma_{rr} = S_{rr} - P; \tag{21}$$

$$P = \frac{1}{3}\left(\sigma_{rr} + \sigma_{\theta\theta} + \sigma_{zz}\right), \tag{22}$$

where ρ is the current density; U is the speed; t is the time; P is the average hydrostatic pressure; r, θ, z are cylindrical coordinates; σ_i, S_i are tensor and deviator components of the stress tensor; $\overline{V} = V / V_0$, V, V_0 are relative, current and initial specific volumes. For detonation products $S_i = 0$. For the components of the deformation speed tensor, there are the relations:

$$\dot{\varepsilon}_r = \frac{\partial U}{\partial r},\ \ \dot{\varepsilon}_\theta = \frac{U}{r},\ \ \dot{\varepsilon}_z = 0. \tag{23}$$

The expansion of the explosion products occurs according to the binomial isentropy, i.e.

$$P = A\rho^{n_0} + B\rho^{\gamma_0 + 1}. \tag{24}$$

The constant values A, B, n_0, γ_0 in the ratio (25) are unambiguously calculated according to the known characteristics of explosives [46].

The initial conditions for this problem are:

$$U = 0,\ \ P = P_{av},\ \rho = \rho_w \text{ at } 0 \le r \le r_0,\ P = \sigma_r = \sigma_\theta = \sigma_z = 0,\ \ \rho = \rho_0 \text{ at } r > r_0. \tag{25}$$

The boundary conditions are: 1) conditions of continuity of speed and stresses at the boundary between the products of an explosion – and the soil; 2) the condition of "no flow", i.e., the speed on the axis of the charge is zero.

Clay was used as soil, the values of physical constants were as follows:

$\rho_{20} = 1000$ kg/m^3, $\rho_{30} = 2650$ kg/m^3, $c_{30} = 4500$ m/s; $\gamma_2 = 7$; $\gamma_3 = 4$; $\rho_0 c_{s^2} = 3 \cdot 10^7$ Pa,

$\rho_0 c_{D^2} = 3.67 \cdot 10^7$ Pa; $m = 3$; $k = -3.7 \cdot 10^9$ Pa; $\gamma_S = 4$; $\gamma_D = 6$; $\gamma_{SR} = 8$, $\eta_D = 1200$ Pa·s.

Lithium trotyl with the following characteristics was used as explosive:

$$P_n = 9.6 \cdot 10^9 \text{ Pa},\ \rho_n = 1600 \text{ kg/m}^3,\ Q = 4.87 \cdot 10^6 \text{ J/m}^2,\ N = 3.12,\ D = 6440 \text{ t/s}.$$

The dependence of the maximum stress σ_r on the relative distance during the explosion of a cylindrical charge in clay is presented in Fig. 5. Black dots and solid lines 1 correspond to the experiment, dashed line 2 – to the calculation according to the model with a constant coefficient of volumetric viscosity at unloading (14), dashed line 3 – to the calculation according to the model with a variable coefficient of volumetric viscosity at unloading (16). The deviations of experimental data and calculations according to the first model are 34%, and according to the second model – do not exceed 11%.

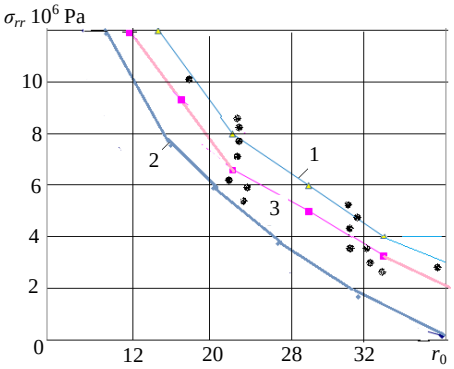

Fig. 5. The dependence of the maximum radial stress σ_r on the relative distances. Black dots and lines 1 – experiment, 2, 3 – calculation by models with a constant variable coefficient of volumetric viscosity during unloading.

This result demonstrates that the model of the soil as a solid porous multicomponent viscoplastic medium with a variable coefficient of viscosity during loading and unloading more adequately describes the wave processes in soils under explosive and dynamic loads than a model with a constant coefficient of viscosity and during unloading.

5 Conclusions

The research investigated the effect of volumetric deformation on the volumetric viscosity coefficient using various loading modes and parameters. The study found that at different dynamic coefficients in viscosity, similar patterns were observed across various soil types. An increase in volumetric deformation led to an increase in the viscosity coefficient, while a higher loading speed resulted in a decrease in this coefficient. The analysis also showed that the coefficient of volumetric viscosity cannot remain constant even when the medium is unloaded, varying significantly based on pressure and deformation conditions. Numerical modeling of explosive impacts in soil demonstrated that a variable viscosity coefficient model more accurately described wave processes compared to a constant viscosity model. This indicates the importance of considering variable viscosity in predicting soil behavior under dynamic loads.

1. It is established that with an increase in volumetric deformation there is an increase in the coefficient of viscosity $\eta(\varepsilon)$, and with an increase in the loading rate, it decreases. In this case, the value $\eta(\varepsilon)$ can be changed on several orders of magnitude. Hence the conclusion follows that even when the medium is unloaded, the coefficient of volumetric viscosity cannot remain constant.

2. Based on the assumption that during unloading, the intermediate unloading diagrams are between the limiting static P_{SR} and dynamic diagrams P_{DR}, and the higher the unloading speed, the closer the curve is to the limiting dynamic diagram, a functional dependence of the viscosity coefficient during soil unloading is obtained.

3. Based on numerous simulations of the explosion of a cylindrical charge of TNT in clay, the calculation results are compared with the experimental data. The result demonstrates that the soil model as a solid porous multicomponent viscoplastic medium with a variable viscosity coefficient during loading and unloading describes wave processes in soils under explosive and dynamic loads more adequately than a model with a constant viscosity coefficient during unloading. The deviation of experimental data and calculation according to the first model is 11%, and according to the second model – does not exceed 34%. The obtained results can be used effectively for the projecting of the protection of shallow underground structures under conditions of dynamic load from explosions, in particular – attacks from the air.

References

1. Novikova, A.M., & Symonenko, R.V. (2022). Sea Ports of Ukraine during the Russian Agression. *European Journal of Maritime Research*, *1*(1), 7-10. https://doi.org/10.24018/maritime.2022.1.1.7
2. Saik, P., Cherniaiev, O., Anisimov, O., Dychkovskyi, R., & Adamchuk, A. (2023). Mining of non-metallic mineral deposits in the context of Ukraine's reconstruction in the war and post-war periods. *Mining of Mineral Deposits*, *17*(4), 91-102. https://doi.org/10.33271/mining17.04.091
3. Polyanska, A., Pazynich, Y., Mykhailyshyn, K., Babets, D., &Toś, P. (2024). Aspects of energy efficiency management for rational energy resource utilization. *Rudarsko-Geološko-NaftniZbornik*, *39*(3), 13-26. https://doi.org/10.17794/rgn.2024.3.2
4. Dychkovskyi, R., Saik, P., Sala, D., & Cabana, E.C. (2024). The current state of the non-ore mineral deposits mining in the concept of the Ukraine reconstruction in the post-war period. *Mineral Economics*, 1-11. https://doi.org/10.1007/s13563-024-00436-z
5. Kicki, J., & Dyczko, A. (2010). The concept of automation and monitoring of the production process in an underground mine. *New Techniques and Technologies in Mining – Proceedings of the School of Underground Mining*, 245-253. https://doi.org/10.1201/b11329-40
6. Sakellariou, M. (Ed.). (2020). *Tunnel Engineering – Selected Topics*. Athens: National Technical University of Athens, 294 p. https://doi.org/10.5772/intechopen.77496
7. Gilbert, P.H., Ariaratnam, S.T., Connery N.R., & English, G. (2013). *Underground Engineering for Sustainble Urban Development*. Washington, DC: The National Academies Press, 246 p. https://doi.org/10.17226/14670
8. Boiko, V.V., Han, A.L., & Han, O.V. (2022). *Spetsialni vybukhovi tekhnolohii v heoinzhenerii*. Kyiv, Ukraina: KPI, 316 s.
9. Tiutkin O.L. (2020). *Teoretychni osnovy kompleksnoho analizu tunelnykh konstruktsii*. Dnipro, Ukraina: Zhurfond, 260 s.
10. Dyczko, A., Galica, D., & Sypniowski, S. (2012). Deposit model as a first step in mining production scheduling. *Geomechanical Processes during Underground Mining – Proceedings of the School of Underground Mining*, 231-247. https://doi.org/10.1201/b13157-39
11. Polyanska, A., Pazynich, Y., Poplavska, Z., Kashchenko, Y., Psiuk, V., & Martynets, V. (2024). Conditions of remote work to ensure mobility in project activity. *Lecture Notes in Mechanical Engineering*, 151-166. https://doi.org/10.1007/978-3-031-56474-1_12
12. Pankratova, N., Haiko, H., & Savchenko, I. (2024). Strategy for modeling complex urban underground environments based on the methodologies of foresight and cognitive modeling. *The Urban Book Series*, 189-256. https://doi.org/10.1007/978-3-031-47522-1_6
13. Dyczko, A., Kamiński, P., Jarosz, J., Rak, Z., Jasiulek, D., & Sinka, T. (2021). Monitoring of roof dolting as an element of the project of the introduction of roof bolting in Polish coal mines – case

study. *Energies*, *15*(1), 95. https://doi.org/10.3390/en15010095

14. Kozachenko, L.S., & Kolkov, O.S. (1976). Shear and bulk deformation in sandy soil. *Soviet Mining Science*, *12*(6), 576-579. https://doi.org/10.1007/bf02497447
15. Russkikh, V., Demchenko, Yu., Salli, S., & Shevchenko, O. (2013). New technical solutions during mining c_5 coal seam under complex hydro-geological conditions of western Donbass. *Annual Scientific-Technical Collection – Mining of Mineral Deposits*, 257-260. https://doi.org/10.1201/b16354-47
16. Geyling, F., & Key, P. (1979). Stress relaxation of residual metalworking stresses. *Stress Relaxation Testing*, 143-154. https://doi.org/10.1520/stp37421s
17. Russkikh, V., Yavors'kyy, A., Zubko, S., & Chistyakov, Ye. (2013). Study of rock geomechanical processes while mining two-level interchamber pillars. *Annual Scientific-Technical Collection – Mining of Mineral Deposits*, 149-152. https://doi.org/10.1201/b16354-25
18. Khoshghalb, A., & Khalili, N. (2014). Coupling between deformation and flow models in deformable unsaturated soils. *Unsaturated Soils: Research & Applications*, 511-516. https://doi.org/10.1201/b17034-71
19. Seheda, M.S., Beshta, O.S., Gogolyuk, P.F., Blyznak, Yu.V., Dychkovskyi, R.D., & Smoliński, A. (2024). Mathematical model for the management of the wave processes in three-winding transformers with consideration of the main magnetic flux in mining industry. *Journal of Sustainable Mining*, *23*(1), 20-39. https://doi.org/10.46873/2300-3960.1402
20. Furuta, T. (1986). Similarity between Kleinecke-Shirokov theorem and Fuglede-Putnam theorem. *Bulletin of the Australian Mathematical Society*, *33*(3), 329-333. https://doi.org/10.1017/s0004972700003890
21. Vladyko, O., Maltsev, D., Sala, D., Cichoń, D., Buketov, V., & Dychkovskyi, R. (2022). Simulation of leaching processes of polymetallic ores using the similarity theorem. *Rudarsko-Geološko-NaftniZbornik*, *37*(5), 169-180. https://doi.org/10.17794/rgn.2022.5.14
22. Psyuk, V., & Polyanska, A. (2024). The usage of artificial intelligence in the activities of mining enterprises. *E3S Web of Conferences*, (526), 01016. https://doi.org/10.1051/e3sconf/202452601016
23. Dyczko, A. (2023). Real-time forecasting of key coking coal quality parameters using neural networks and artificial intelligence. *Rudarsko-Geološko-Naftni Zbornik*, *38*(3), 105-117. https://doi.org/10.17794/rgn.2023.3.9
24. Dychkovskyi, R., Tabachenko, M., Zhadiaieva, K., & Cabana, E. (2019). Some aspects of modern vision for geoenergy usage. *E3S Web of Conferences*, (123), 01010. https://doi.org/10.1051/e3sconf/201912301010
25. Dudek, M., & Pawlewski, P. (2010). Implementation of Network oriented manufacturing structures. *Lecture Notes in Computer Science*, 282-291. https://doi.org/10.1007/978-3-642-13541-5_29
26. Meschyan, S.R. (1967). *Clay soil creep*. Yerevan: Barekamutyan, 320 p.
27. Meschyan, S.R. (2005). *Experimental rheology of claysoils*. Yerevan: Gitutyun NANRA, 498 p.
28. Shirinkulov, T.Sh., & Zareckij, Yu.K.(1986). *Creep and soil consolidation.* Tashkent: FAN Uzbekskij SSR, 392 p.
29. Ter-Martirosyan, Z., Ter-Martirosyan, A., & Ermoshina, L. (2022). Settlement and long-term bearing capacity of a pile taking into account the rheological properties of soils. *Construction and Geotechnics*, *13*(1), 5-15. https://doi.org/10.15593/2224-9826/2022.1.01
30. Grant, K. (1982). Fundamentals of Soil Physics. *Engineering Geology*, *19*(1), 70. https://doi.org/10.1016/0013-7952(82)90012-6
31. Meschyan, S.R. (1992). *Rheological processes in clayey soils (taking into account special influences).* Yerevan: Hayastan, 395 p.
32. Bell, F.G. (1983). The mechanics of soil. *Fundamentals of Engineering Geology*, 373-434. https://doi.org/10.1016/b978-0-408-01169-3.50013-4

33. Savon, D.Yu., Zhaglovskaya, A.V., Safronov, A.E., & Sala, D. (2018). Development of patenting in coal industry. *Eurasian Mining*, 9-11. https://doi.org/10.17580/em.2018.01.02
34. Pedchenko, M., Pedchenko, L., Nesterenko, T., & Dyczko, A. (2018). Technological Solutions for the Realization of NGH-Technology for Gas Transportation and Storage in Gas Hydrate Form. *Solid State Phenomena*, (277), 123-136. https://doi.org/10.4028/www.scientific.net/ssp.277.123
35. Nieuwenhuis, J.D. (1988). Rheological Fundamentals of Soil Mechanics. *Engineering Geology*, *26*(1), 102. https://doi.org/10.1016/0013-7952(88)90009-9
36. Sobolev, E., & Morev, D. (2019). The industrial buildings settlement foundations calculation made taking into account the soils vibro-creep. *IOP Conference Series: Materials Science and Engineering*, *698*(2), 022038. https://doi.org/10.1088/1757-899x/698/2/022038
37. Arenson, L.U., Springman, S.M., & Sego, D.C. (2007). The Rheology of Frozen Soils. *Applied Rheology*, *17*(1), 12147-1-12147-14. https://doi.org/10.1515/arh-2007-0003
38. Zaretskii, Yu., & Fish, A.(1996). Effect of temperature on the strength and viscosity of ice. *Soil Mechanics and Foundation Engineering*, (33), 46-52.
39. Tatsuoka, F., Di Benedetto, H., Enomoto, N., Kawabe, S., & Kongkitkul, W. (2008). Variousviscositytypesofgeomaterialsinshearandtheirmathematicalexpression. *Soils and Foundations*, *48*(1), 41-60.
40. Naumenko, N., Markova, O., Kovtun E., & Maly, V. (2015). Determination of deformation of the soil foundation under the influence of short-term load. *Technical mechanics*, 261 p.
41. Dyczko, A., Kamiński, P., Steculа, K., Prostański, D., Kopacz, M., & Kowol, D. (2021). Thermal and mechanical energy storage as a chance for energy transformation in Poland. *Polityka Energetyczna – Energy Policy Journal*, *24*(3), 43-60. https://doi.org/10.33223/epj/141867
42. Sultanov, K., Loginov, P., Ismoilova, S., & Salikhova, Z. (2019). Wave processes in determining mechanical characteristics of soils. *E3S Web of Conferences*, (97), 04009. https://doi.org/10.1051/e3sconf/20199704009
43. Bai, M., & Elsworth, D. (1995). On the modeling of miscible flow in multi-component porous media. *Transport in Porous Media*, *21*(1), 19-46. https://doi.org/10.1007/bf00615333
44. Remez, N.S. (2019). *Vzaiemodiia vybukhovukh khvyl z hruntamy i elementamy tekhnourboekosystem*. Kyiv, Ukraina: Tsentr uchbovoi literatury, 335.
45. Remez, N., Dychko, A., Besarabets, Y., Kraychuk, S., Ostapchuk, N., & Yevtieieva, L. (2019). Impact modelling of explosion of mixture explosive charges on the environment. *Latvian Journal of Physics and Technical Sciences*, *56*(3), 37-49. https://doi.org/10.2478/lpts-2019-0018
46. Remez, N., Dychko, A., Bronytskyi, V., Hrebeniuk, T., Bambirra Pereira, R., & Ekel, P. (2021). Simulation of the influence of dynamic loading on the stress-strain state of the natural and geoengineering environment. *E3S Web of Conferences*, (280), 01008. https://doi.org/10.1051/e3sconf/202128001008